

Supporting Information

Insights on Seed Selection Criteria of SAPO-34 Synthesis: Structure Units and Chemical Microenvironment

*Xiaosi Zhang,^{ab} Miao Yang,^{*a} Ye Wang,^{ac} Caiyi Lou,^{ab} Shutao Xu,^a Peng Tian^{*a} and
Zhongmin Liu^{ab}*

^a National Engineering Research Center of Lower-Carbon Catalysis Technology, Dalian National Laboratory for Clean Energy, iChEM (Collaborative Innovation Center of Chemistry for Energy Materials), Dalian Institute of Chemical Physics, Chinese Academy of Sciences, Dalian 116023, (P. R. China)

^b University of Chinese Academy of Sciences, Beijing 100049, (P. R. China)

^c Green Catalysis Centre, College of Chemistry, Zhengzhou University, Zhengzhou 450001, (P. R. China)

*Corresponding authors: yangmiao@dicp.ac.cn; tianpeng@dicp.ac.cn

Table of Contents

1. Supplementary Tables

Table S1. The collections of various seeds.

Table S2. Textural properties of the seeds.

Table S3. Textural properties of the samples for the MTO evaluation.

2. Supplementary Figures

Fig. S1. The powder XRD patterns and SEM images of relevant products.

Fig. S2. The SEM images of SAPO-34 seeds with different Si contents and the corresponding seed-assisted synthesis products.

Fig. S3. XRD patterns of the products synthesized without seed and seeded by **CHA-0.20-2** with different reaction times, and SEM images of the products seeded by **CHA-0.20-2**.

Fig. S4. The similarity between different topology structures and **CHA**.

Fig. S5. The SEM images of seed AlPO-18 (**AEI-0-0.5**) and SAPO-18 (**AEI-0.03-0.5**), and XRD patterns of the products seeded by AlPO-18 (**AEI-0-0.5**) and SAPO-18 (**AEI-0.03-0.5**).

Fig. S6. The powder XRD patterns and the solid yields of the products assisted by seeds without **d6r** units in a concentrated MOR-templated system.

Fig. S7. Solid-state ^{29}Si MAS NMR spectra for the calcined SAPO seeds without **d6r** units in their structures.

Fig. S8. The XRD patterns and SEM images of the samples for the MTO evaluation.

3. References

1. Supplementary Tables

Table S1 The collections of various seeds.

Seed samples	Gel molar composition SiO ₂ /Al ₂ O ₃ /P ₂ O ₅ /H ₂ O/R	T/°C	t/h	Elemental composition	
				Measured by XRF	SAR ^a
CHA-0.19-0.5	1 SAPO-34-BM:4 DEA:0.4 H ₂ O (mass ratio)	200	2	Al _{0.508} Si _{0.187} P _{0.305} O ₂	0.37
CHA-0.20-2 ¹	0.31/1/1/100/1.5 PIP/4.5 TEA (seed) ^b	200	24	Al _{0.459} Si _{0.199} P _{0.341} O ₂	0.43
CHA-0.19-10 (MS)	1/1/0.8/100/2.5 MOR	200	24	Al _{0.468} Si _{0.191} P _{0.341} O ₂	0.41
CHA-0-0.5 (MS)	0/1/1/50/2.5 Py/0.4 HF	200	24	Al _{0.505} P _{0.495} O ₂	0
CHA-0.06-1 ²	0.2/0.8/1/50/1.8 TEA/1.5 TEABr	120	96	Al _{0.491} Si _{0.062} P _{0.447} O ₂	0.13
CHA-0.10-2 (MS)	0.6/1/0.8/100/2.5 MOR (seed) ^b	200	2	Al _{0.505} Si _{0.100} P _{0.395} O ₂	0.20
CHA-0.15-1 ³	0.75/1/1/50/0.4 TEOH/2.6 TEA	200	24	Al _{0.458} Si _{0.145} P _{0.398} O ₂	0.32
CHA-0.91-0.5 ⁴	20/10/0/440/2.0 TMAOH/1.0 Na ₂ O	160	96	Al _{0.09} Si _{0.91} O ₂	10.13
LEV-0.18-5 ⁵	0.5/1.0/0.96/55/1.35 HMI	200	25	Al _{0.457} Si _{0.175} P _{0.368} O ₂	0.38
AFX-0.22-8 ⁶	0.6/0.8/1.0/50/2.0 TMHDA	200	48	Al _{0.437} Si _{0.222} P _{0.341} O ₂	0.51
AEI-0.07-1 ⁷	0.4/1/1/50/1.8 DIEA	160	48	Al _{0.513} Si _{0.066} P _{0.421} O ₂	0.13
AEI-0.03-0.5 ⁷	0.1/1/1/50/2 DIEA	160	65	Al _{0.498} Si _{0.032} P _{0.470} O ₂	0.06
AEI-0-0.5 ⁸	0/1/1/50/1.8 DIEA	160	24	Al _{0.518} P _{0.482} O ₂	0
LTA-0.17-1 ⁹	0.35/0.5/0.4/50/2.0 DPA/0.15 C ₁₆ TAB	200	24	Al _{0.463} Si _{0.168} P _{0.369} O ₂	0.35
RHO-0.25-0.5 ¹⁰	0.6/0.5/0.4/50/1.5 DEA/0.2 C ₁₈ TAB	200	24	Al _{0.444} Si _{0.253} P _{0.303} O ₂	0.57
RHO-0.33-8 ¹¹	1.7/1.0/1.0167.0/5.0 DMEDA	200	12	Al _{0.444} Si _{0.332} P _{0.224} O ₂	0.75
SOD-0.18-0.3 ¹²	1.0/1.0/1.0/60/1.5 TMAOH/1.0 TMEDA	200	24	Al _{0.499} Si _{0.183} P _{0.318} O ₂	0.37

a SAR refers to the Si/Al molar ratio.

b The seed used here was SAPO-34-BM, and the nominal amount of seeds used in experiments was 5wt % (calculated relative to the total mass of oxides in the gel).

Table S2. Textural properties of the seeds.

Seeds	Surface area (m ² g ⁻¹) ^a			Pore volume (cm ³ g ⁻¹) ^b	
	S _{total}	S _{micro}	S _{ext}	V _{mic}	V _{total}
SAPO-34-BM	51.42	28.07	23.35	0.013	0.079
AFX-0.22-8 (SAPO-56)	494.28	433.94	60.35	0.211	0.296
LEV-0.18-5 (SAPO-35)	521.22	475.41	45.82	0.222	0.285
AEI-0.07-1 (SAPO-18)	508.68	482.72	25.96	0.237	0.300

a S_{total}: BET surface area; S_{micro}: t-plot micropore surface area; S_{ext}=S_{total} - S_{micro}.

b V_{total} is evaluated at P/P₀=0.97; V_{micro}=t-plot micropore volume.

Table S3. Textural properties of the samples for the MTO evaluation.

Samples	Surface area ($\text{m}^2 \text{g}^{-1}$) ^a			Pore volume ($\text{cm}^3 \text{g}^{-1}$) ^b	
	S_{total}	S_{micro}	S_{ext}	V_{mic}	V_{total}
S-0.6-8h	484.9	484.8	0.13	0.244	0.247
$S_{\text{AFX-0.22-8-2h}}$	494.7	492.7	2.0	0.260	0.305
$S_{\text{AEI-0.07-1-8h}}$	546.5	544.6	1.9	0.268	0.279

a S_{total} : BET surface area; S_{micro} : t-plot micropore surface area; $S_{\text{ext}}=S_{\text{total}} - S_{\text{micro}}$.

b V_{total} is evaluated at $P/P_0=0.97$; V_{micro} =t-plot micropore volume.

2. Supplementary Figures

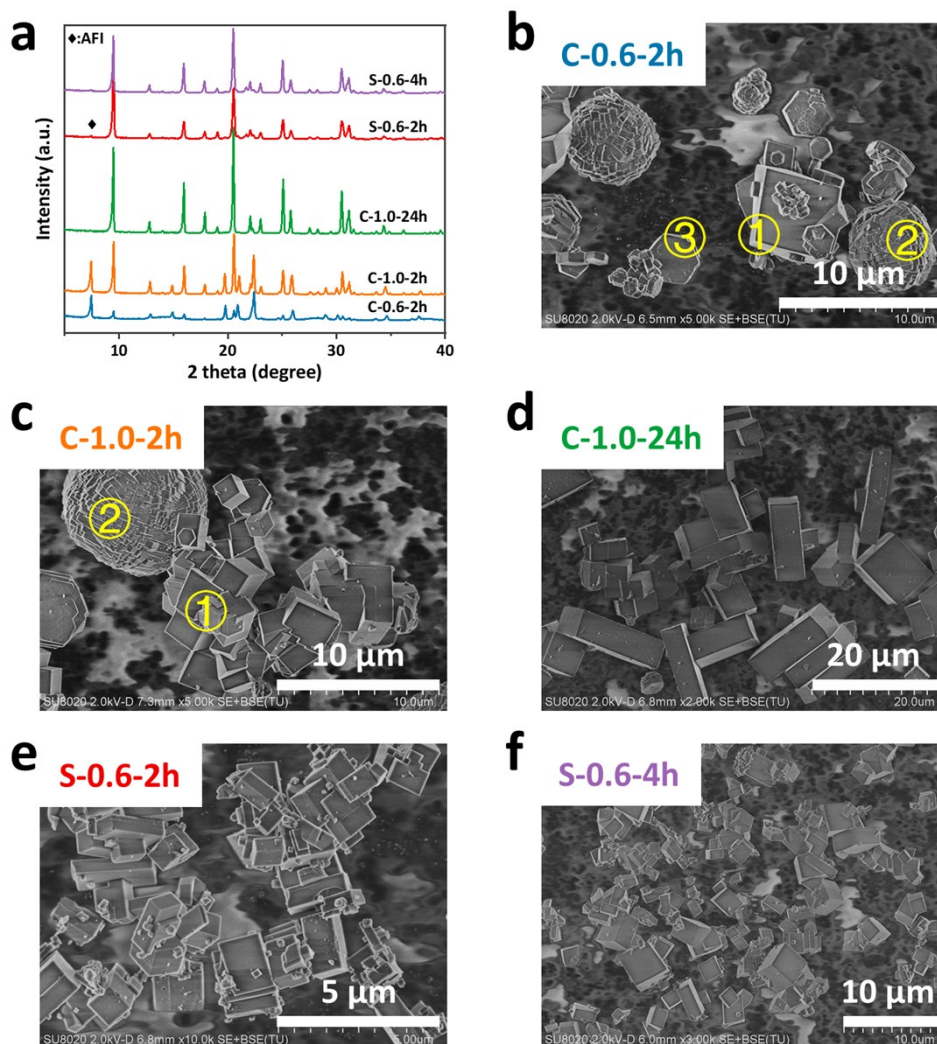


Fig. S1. (a) The powder XRD patterns and (b-f) SEM images of relevant products. The numbers inserted in b and c represent different crystal phases. The statistical averages of elemental compositions for C-0.6-2h: ① $\text{Al}_{0.511}\text{Si}_{0.102}\text{P}_{0.387}\text{O}_2$, ② $\text{Al}_{0.530}\text{Si}_{0.045}\text{P}_{0.425}\text{O}_2$, ③ $\text{Al}_{0.529}\text{Si}_{0.042}\text{P}_{0.430}\text{O}_2$; for C-1.0-2h, ① $\text{Al}_{0.513}\text{Si}_{0.106}\text{P}_{0.381}\text{O}_2$, ② $\text{Al}_{0.503}\text{Si}_{0.057}\text{P}_{0.440}\text{O}_2$.

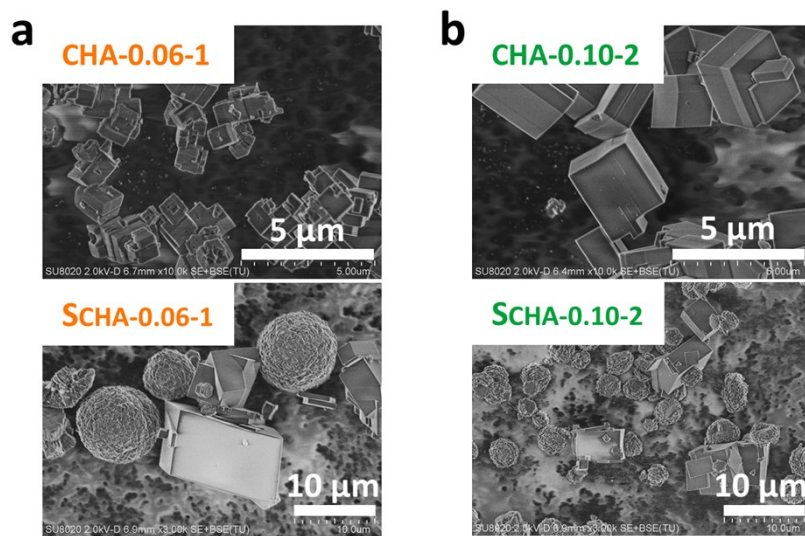


Fig. S2. The SEM images of SAPO-34 seeds with different Si contents (top) and the corresponding seed-assisted synthesis products (bottom).

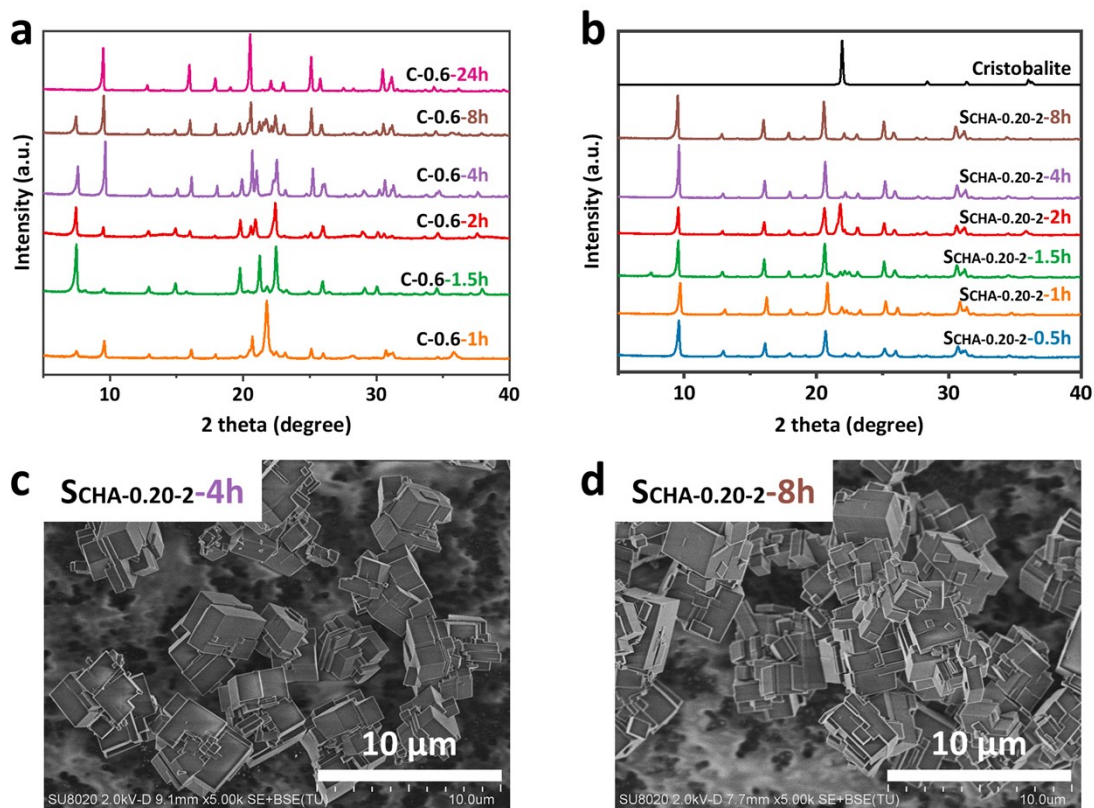


Fig. S3. XRD patterns of the products synthesized without seed (a) and seeded by **CHA-0.20-2** (b) with different reaction times, and SEM images (c, d) of the products seeded by **CHA-0.20-2**. (Note: There was no solid product after 0.5 h without seed.)

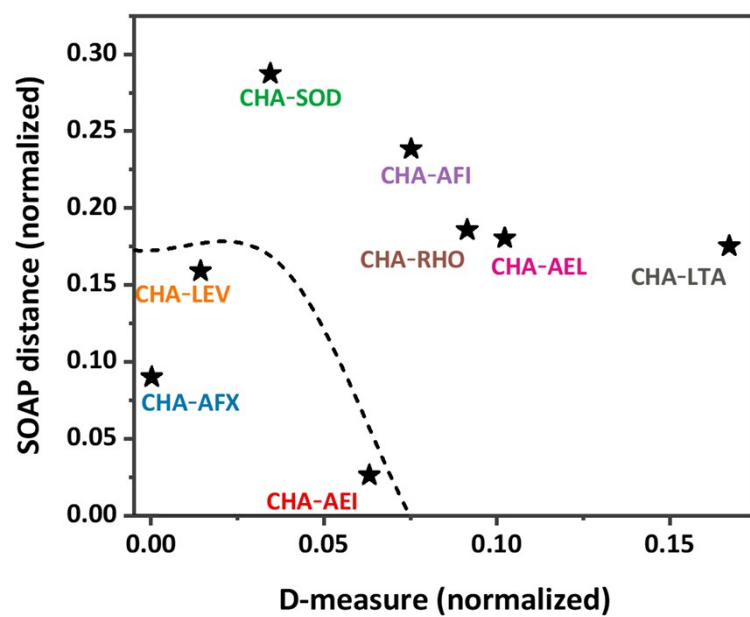


Fig. S4. The similarity between different topology structures and CHA^{13} .

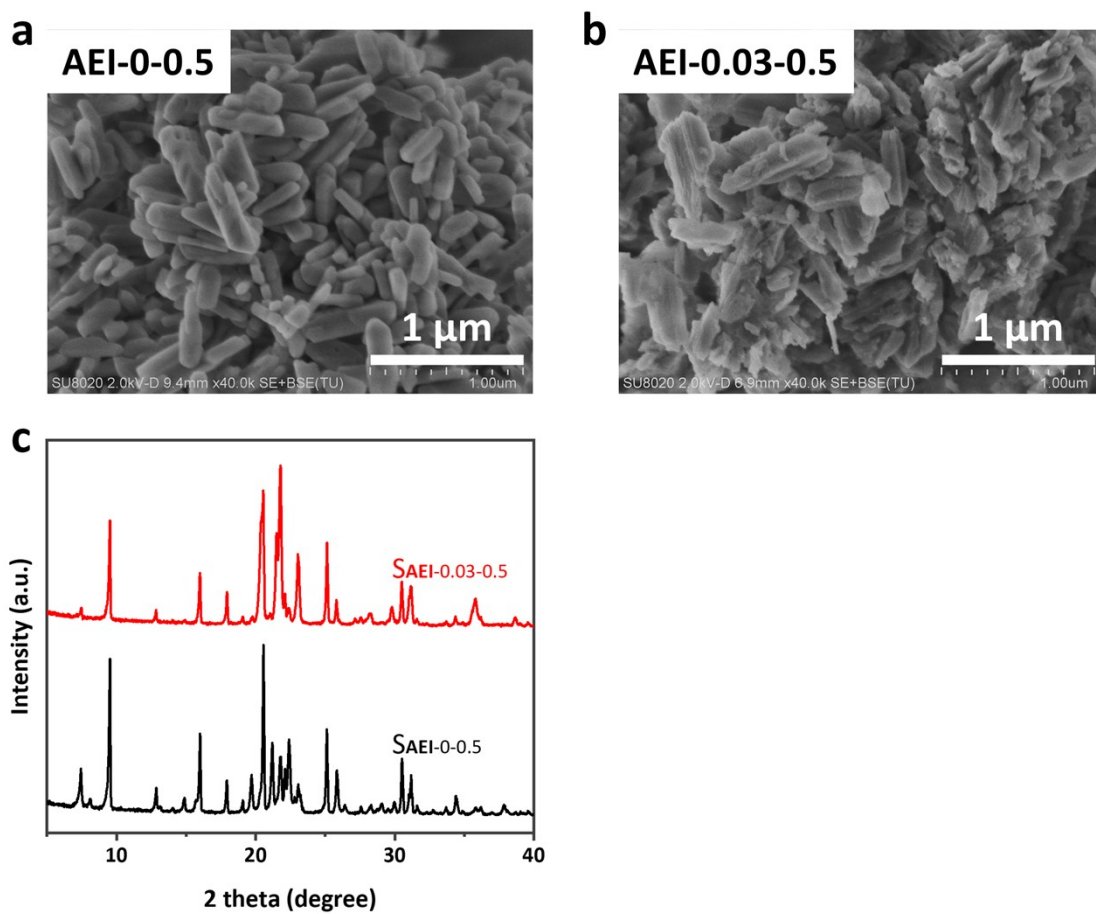


Fig. S5. The SEM images of seed (a) AIPO-18 (**AEI-0-0.5**) and (b) SAPO-18 (**AEI-0.03-0.5**), and (c) XRD patterns of the products seeded by AIPO-18 (**AEI-0-0.5**) and SAPO-18 (**AEI-0.03-0.5**). The gel composition and synthesis condition were the same as sample S-0.6-8h except the variation of seeds.

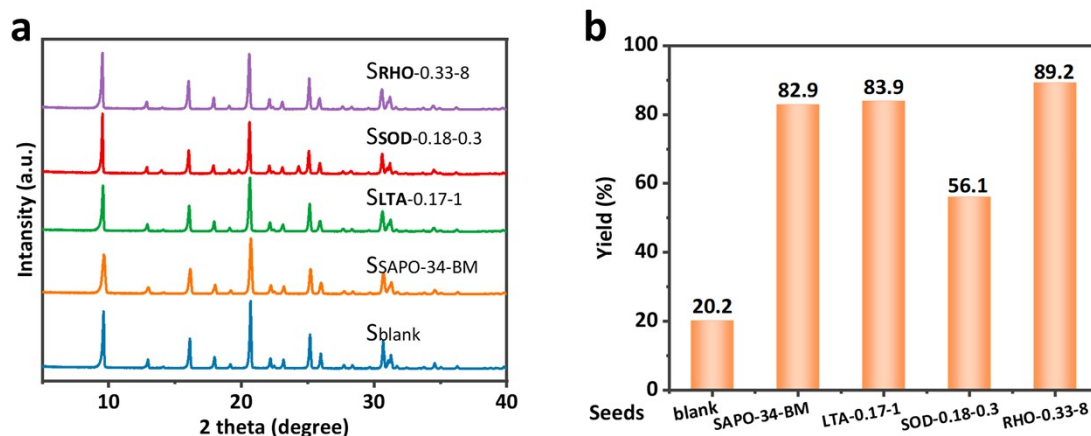


Fig. S6. The powder XRD patterns (a) and the solid yields (b) of the products assisted by seeds without *d6r* units in a concentrated MOR-templated system. Gel molar composition: $0.8\text{P}_2\text{O}_5$: $1.0\text{Al}_2\text{O}_3$: 0.6SiO_2 : 2.5MOR : $50.0\text{H}_2\text{O}$ (5wt % addition of seeds based on oxide dry mass at $200\text{ }^\circ\text{C}$ for 2 h).

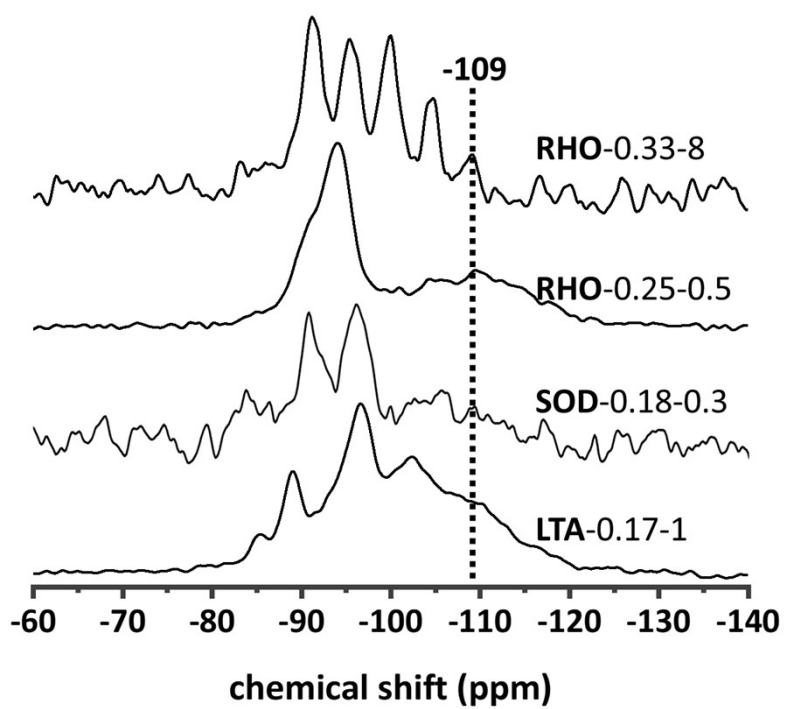


Fig. S7. Solid-state ^{29}Si MAS NMR spectra for the calcined SAPO seeds without *d6r* units in their structures.

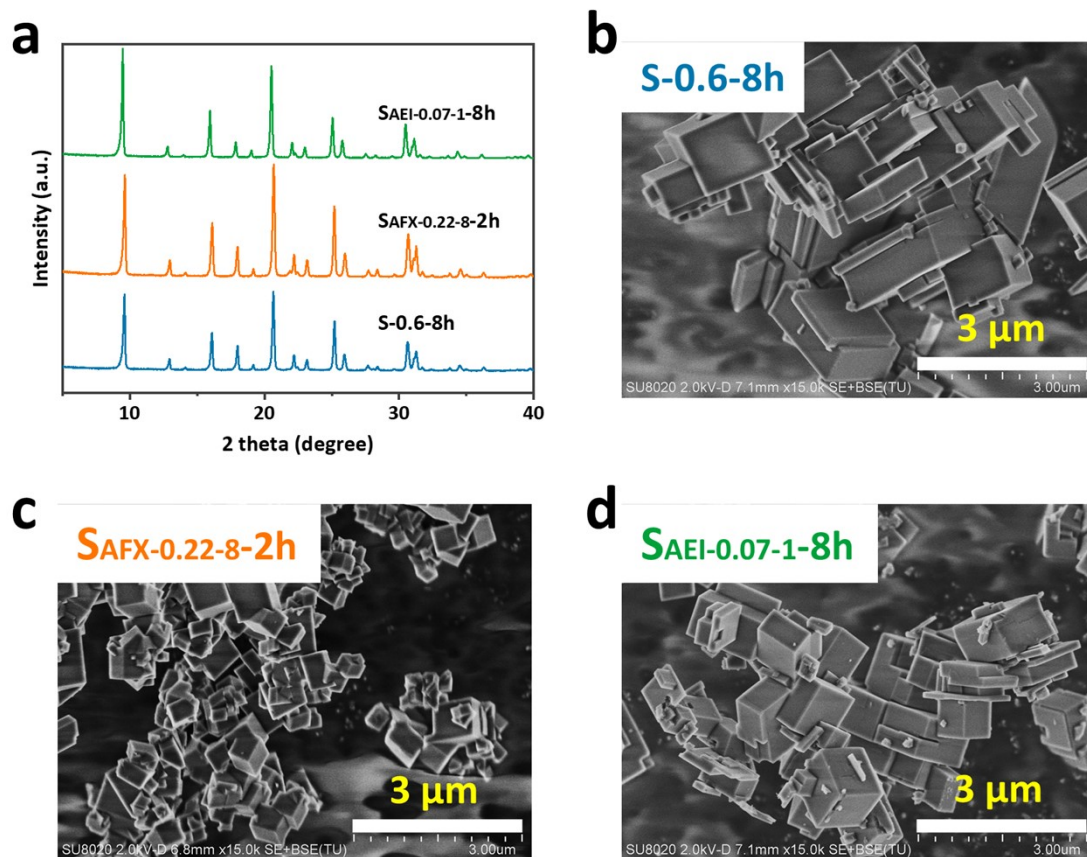


Fig. S8. The XRD patterns (a) and SEM images (b-d) of the samples for the MTO evaluation.

3. References

1. P. F. Wu, M. Yang, L. J. Sun, S. Zeng, S. T. Xu, P. Tian and Z. M. Liu, Synthesis of nanosized SAPO-34 with the assistance of bifunctional amine and seeds, *Chem. Commun.*, 2018, **54**, 11160-11163.
2. B. B. Gao, M. Yang, Y. Y. Qiao, J. Z. Li, X. Xiang, P. F. Wu, Y. X. Wei, S. T. Xu, P. Tian and Z. M. Liu, A Low-Temperature Approach to Synthesize Low-Silica SAPO-34 Nanocrystals and their Application in the Methanol-to-Olefins (MTO) Reaction, *Catal. Sci. Technol.*, 2016, **6**, 7569-7578.
3. Y. Cao, D. Fan, D. Zhu, L. Sun, L. Cao, P. Tian and Z. Liu, The effect of Si environments on NH₃ selective catalytic reduction performance and moisture stability of Cu-SAPO-34 catalysts, *J. Catal.*, 2020, **391**, 404-413.
4. F. Gao, N. M. Washton, Y. L. Wang, M. Kollár, J. Szanyi and C. H. F. Peden, Effects of Si/Al ratio on Cu/SSZ-13 NH₃-SCR catalysts: Implications for the active Cu species and the roles of Brønsted acidity, *J. Catal.*, 2015, **331**, 25-38.
5. P. Tian, B. Li, S. T. Xu, X. Su, D. H. Wang, L. Zhang, D. Fan, Y. Qi and Z. M. Liu, Investigation of the Crystallization Process of SAPO-35 and Si Distribution in the Crystals, *J. Phys. Chem. C*, 2013, **117**, 4048-4056.
6. P. Tian, L. Xu, Z. M. Liu, C. L. Sun and T. Huang, Synthesis and Characterization of SAPO-56, a New Member of Silicoaluminophosphate, *Chem. J. Chinese Universities*, 2001, **22**, 991-994.
7. D. Fan, Y. Qiao, K. Cao, L. Sun, S. Xu, P. Tian and Z. Liu, Preparation of Hierarchical SAPO-18 via alkaline/acid etching, *Microporous Mesoporous Mater.*, 2020, DOI: 10.1016/j.micromeso.2020.110156, 110156.
8. J. S. Chen, P. A. Wright, J. M. Thomas, S. Natarajan, L. Marchese, S. M. Bradley, G. Sankar, C. R. A. Catlow, P. L. Gaiboyes, R. P. Townsend and C. M. Lok, SAPO-18 Catalysts and Their Bronsted Acid Sites, *J. Phys. Chem.*, 1994, **98**, 10216-10224.
9. N. Yan, L. Wang, X. Liu, P. Wu, T. Sun, S. Xu, J. Han, P. Guo, P. Tian and Z. Liu, A Novel Approach for Facilitating the Targeted Synthesis of Silicoaluminophosphates, *J. Mater. Chem. A*, 2018, **6**, 24186-24193.
10. M. Yang, P. Tian, L. Liu, C. Wang, S. Xu, Y. He and Z. Liu, Cationic surfactant-assisted hydrothermal synthesis: an effective way to tune the crystalline phase and morphology of SAPO molecular sieves, *CrystEngComm*, 2015, **17**, 8555-8561.
11. P. Wu, M. Yang, W. Zhang, S. Zeng, M. Gao, S. Xu, P. Tian and Z. Liu, Silicoaluminophosphate Molecular Sieve DNL-6: Synthesis with a Novel Template, N,

N'-dimethylethylenediamine, and Its Catalytic Application, *Chin. J. Catal.*, 2018, **39**, 1511-1519.

12. Y. Qiao, M. Yang, B. Gao, L. Wang, P. Tian, S. Xu and Z. Liu, Creation of Hollow SAPO-34 Single Crystals via Alkaline or Acid Etching, *Chem. Commun.*, 2016, **52**, 5718-5721.

13. D. Schwalbe-Koda, Z. Jensen, E. Olivetti and R. Gomez-Bombarelli, Graph similarity drives zeolite diffusionless transformations and intergrowth, *Nat. Mater.*, 2019, **18**, 1177-1181.